



Fiber array to chip attach using laser fusion splicing for low loss

JUNIYALI NAURIYAL,¹ MEITING SONG,² YI ZHANG,² MARISSA GRANADOS-BAEZ,² AND JAIME CARDENAS^{2,3,*}

¹Department of Electrical and Computer Engineering, University of Rochester, Rochester, NY 14627, USA

²The Institute of Optics, University of Rochester, Rochester, NY 14627, USA

³Department of Physics and Astronomy, University of Rochester, Rochester, NY 14627, USA

*jaime.cardenas@rochester.edu

Abstract: With the ever-increasing need for higher data rates, datacom and telecom industries are now migrating to silicon photonics to achieve higher data rates with reduced manufacturing costs. However, the optical packaging of integrated photonic devices with multiple I/O ports remains a slow and expensive process. We introduce an optical packaging technique to attach fiber arrays to a photonic chip in a single shot using CO₂ laser fusion splicing. We show a minimum coupling loss of 1.1 dB, 1.5 dB, and 1.4 dB per-facet for 2, 4, and 8-fiber arrays (respectively) fused to the oxide mode converters using a single shot from the CO₂ laser.

© 2023 Optica Publishing Group under the terms of the [Optica Open Access Publishing Agreement](#)

Due to the need for high-bandwidth communication systems, more efficient data processing, and the growing demand for sensors, companies are now migrating to silicon photonics for achieving higher data rates with low loss and reduced thermal extraction costs. The field of co-packed optics is predicted to use an average 16 I/O ports per chip, with a multi-chip layout [1–4]. However, the optical packaging of silicon photonic devices with multiple I/O ports remains a slow and expensive process. A low-loss packaging technique for photonic integrated circuits that can be scaled to high volume manufacturing is required to keep up with increasing data traffic. With the introduction of co-packaged optics, optics onboard, [1,5,6] and pluggable high-speed optical transceivers, multiple I/O ports will become the norm as the parallelism between electronics and optics grows [2]. As integrated photonic devices become more complex needing multiple I/O ports, fiber-arrays or ribbon fibers are used instead of a single optical fiber. Increase in the number of I/O is leading to increased packaging times and alignment complexities [2,7–9]. To advance integrated photonic devices and to achieve manufacturing scalability we need high performance devices with multiple I/O ports. Current packaging techniques for multiple fibers rely on attaching one fiber at a time or fiber-array units using adhesives, flip-chip bonding, die bonding, photonic wire bonding, v-grooves with MP connectors, or using fiber blocks in conjunction with micro-optics [1,8–20]; however, these packaging methods are slow and increase the overall device loss. The current state of the art insertion loss for a two fiber array attachment technique is >1.3 dB [8]. Most of these packaging methods rely on optical adhesives to package single/multiple fibers to a photonic chip after active or passive alignment between the fiber and the chip. In this paper, we refer to the process of attaching an optical fiber/fiber array to a photonic chip as “fiber-attach”.

We introduce an optical packaging technique to attach fiber arrays to a photonic chip in a single shot using CO₂ laser fusion splicing. We use laser fusion splicing to permanently attach a fiber array to a photonic chip with oxide mode converters [21] as shown in Fig. 1. The fiber-attach process consists of two steps. First, we use an oxide mode converter [21] to improve the coupling between the fibers in the array and the waveguides on the photonic chip. The oxide mode converter helps in matching the modes between the SMF-28 optical fiber (mode size of 10.4 μ m) to a waveguide nanotaper (mode size 2~5 μ m). We engineer the geometry of the two sides of the

oxide mode converter to maximize the coupling from the waveguide nanotaper to the cleaved optical fiber. To provide mechanical stability and avoid misalignment of the fiber arrays we introduce u-grooves [22] on the chip. Second, we use a CO₂ laser to form a fusion bond between the oxide mode converter and the optical fiber array. The laser fusion splicing process is low-loss, low-cost, resilient, and scalable to high-volume manufacturing. Since both the fiber and the chip have a cladding of silicon dioxide, we use a laser to heat the silicon dioxide cladding on the chip and the optical fiber to their glass transition temperature and fuse them permanently. Due to the formation of the glass-to-glass bond between the optical fiber array and the oxide mode converter on the photonic chip, losses from surface reflections are minimized. The misalignment tolerance increases due to the enlarged mode size.

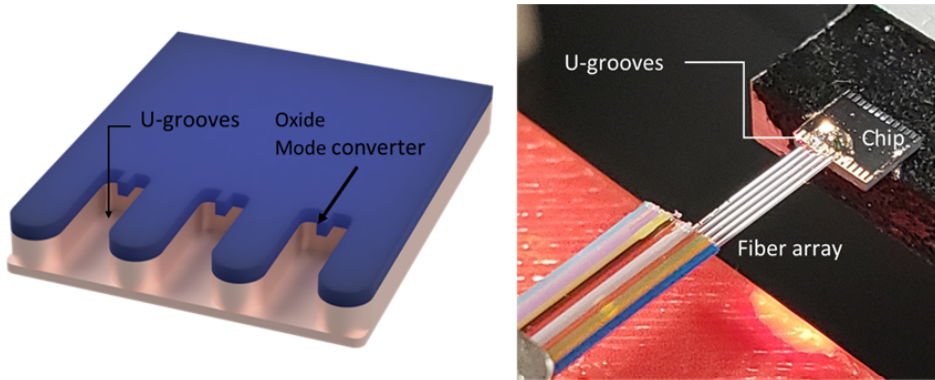


Fig. 1. 3D illustration of a photonic chip with buried SiN waveguides, SiO₂ mode converters and u-grooves for attaching fiber arrays (left), and photographic image of a chip attached to a ribbon fiber using laser fusion splicing.

We fabricate a silicon nitride photonic chip using standard, CMOS-compatible, microfabrication techniques. To achieve maximum coupling, a total oxide cladding thickness of 11 μm was selected [21]. We deposit a 5.5 μm layer of silicon dioxide via plasma-enhanced chemical vapor deposition (PECVD) and 305 nm of silicon nitride via low-pressure chemical vapor deposition (LPCVD). The waveguides with inverse tapers [23] are patterned using standard DUV optical lithography at 248 nm using an ASML PAS 5500/300C DUV Wafer Stepper on the silicon nitride layer. The waveguides are looped with a pitch of 250 μm for testing with a fiber array and have u-grooves that are 170 μm long and 127 μm wide for a single mode fiber as shown in Fig. 2. After etching in an inductively coupled plasma reactive ion etcher (ICP-RIE) with CHF₃/O₂ chemistry, the devices are clad with 5.6 μm of oxide using a plasma-enhanced chemical vapor deposition (PECVD). We then pattern and etch the oxide mode converter similarly to the waveguide step. The optimum dimensions of the oxide mode converter are selected based on the coupling loss simulations for TE polarized light between a silicon nitride waveguide nanotaper and the optical fiber using the eigenmode expansion method (FIMMPROP by Photon Design) with mode overlaps.

The eigenmode simulations, as shown in Fig. 3, show the total transmission loss between an SMF-28 fiber, silicon dioxide mode converter, and the silicon nitride waveguide nanotaper. To obtain the lowest transmission loss throughout the device we optimize the input and output width of the oxide mode converter for a fixed oxide cladding thickness (11 μm), waveguide taper width (0.1 μm -0.3 μm), and input fiber mode (10.4 μm). The simulations show that for an input mode converter width between 11 μm and 14 μm , for a silicon nitride waveguide taper width ranging between 200 nm to 250 nm and fixed output mode converter width of 12 μm , the total transmission loss is 0.5 dB. Similarly, for an output mode converter width between 11 μm to 13.5 μm , the total transmission loss is 0.5 dB for a fixed input width of 12.5 μm . An oxide mode

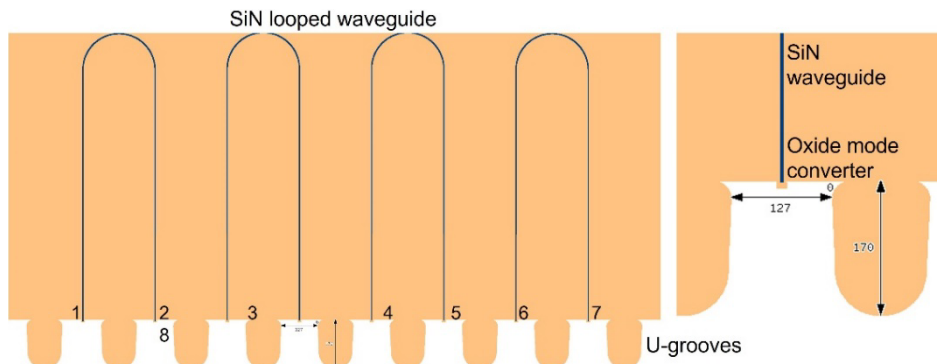


Fig. 2. Schematic of the designed photonic chip with oxide mode converters introduced at the edge of waveguide loopbacks and u-grooves for alignment of fiber arrays.

converter as shown in Fig. 2 with an input mode converter width of $12\mu\text{m}$, an output mode converter width of $13\mu\text{m}$, and a length of $10\mu\text{m}$ is photolithographically patterned with the chip layout. The chip layout has u-grooves which are $127\mu\text{m}$ wide with a $250\mu\text{m}$ pitch. The oxide mode converters, waveguide tapers, and u-grooves are centered with each other. Each photonic chip has 8 individual oxide mode converters with 8 u-grooves to test and package an 8-fiber array. We then pattern the chip structure with u-grooves and deep-etch the silicon to a depth of $100\mu\text{m}$ - $120\mu\text{m}$. After dicing, we remove the silicon substrate using xenon difluoride (XeF_2) dry etch to optically isolate the oxide mode converter from the silicon substrate.

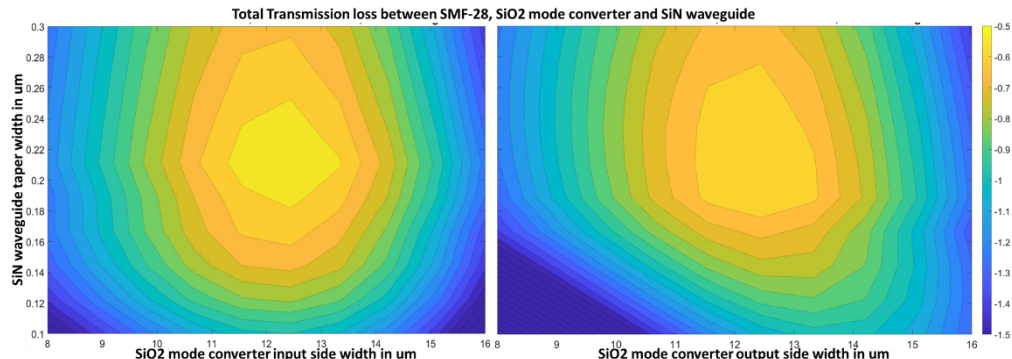


Fig. 3. Simulations for optimum dimensions of the silicon dioxide mode converter for different waveguide taper widths, and mode converter taper widths.

We fuse 2, 4, and 8 SMF-28 fiber arrays with a mode field diameter of $10.4\mu\text{m}$ to the photonic chip at the oxide mode converter interface using a CO₂ laser($10.6\mu\text{m}$) in a single shot. The optical fiber array is fused to the oxide mode converter via radiative heating, as silicon dioxide readily absorbs light at a wavelength of $10.6\mu\text{m}$. Because the fusing of the fiber to the chip is radiative, losses from the splicing residues such as small amount of fiber material that remains after the fusion are minimized, and a glass-to-glass bond is formed [24]. To fuse all the fibers in the array in one shot (rather than one at a time), we use a cylindrical lens to focus the beam of the CO₂ laser in one dimension to a width of 3 mm and $50\mu\text{m}$ (width of a 12-fiber array).

The beam is focused into a line at the chip fiber interface and aligned at the fiber array to the oxide mode converter interface (Fig. 4) and then radiated with a CO₂ laser for 2 seconds at 20W /-2W of laser power [25–27]. The beam width (3 mm) is selected to enable fusing a 12-fiber array

in a single shot for future applications. The fiber array used for fusion splicing is an 8-fiber array with fibers extending 2 mm from the edge of the v-groove glass block with a glass lid to decrease misalignment of the fiber cores. The size of the beam can be modified by using a cylindrical lens of the appropriate focal length. The laser beam is incident at an angle of 30°, which gives a clear line of sight to the full chip facet. Fusing multiple fibers at once significantly decreases the time (here 8 times when compared to one at a time single fiber attach) and the cost involved in optical packaging of a single chip and is scalable for manufacturing. The laser fusion splicing process between the fiber array and the chip using radiative heating forms a permanent bond and decreases coupling losses by eliminating the Fresnel reflections at both oxide–air interfaces and the gap between the fiber array and the oxide mode converter. We did not observe a decrease in optical power through the waveguide after fusion splicing indicating that the heat from the laser fusion process did not damage the waveguide. We observe that long fusion times (>5s) can cause damage and misalignment of the fiber due to thermal shock.

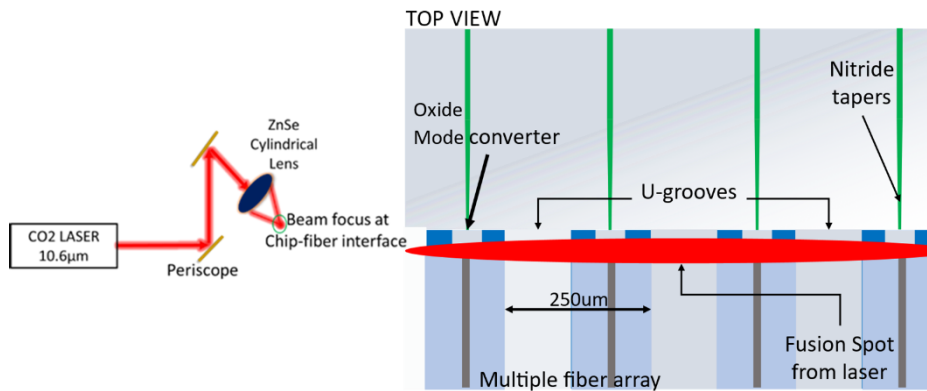


Fig. 4. Setup for fusion splicing between a 12-fiber array and a photonic chip with oxide mode converters using a cylindrical lens for focusing (right), top view of photonic chip (left).

We show a minimum coupling loss of 1.1 dB, 1.5 dB and 1.4 dB per-facet for 2, 4 and 8-fiber arrays (respectively) fused to the oxide mode converters using a single shot from the CO₂ laser. To measure the coupling loss across an 8-fiber array, the device consists of 8 waveguides that are looped internally on the chip with a 1-2, 3-4, 5-6, 7-8 pattern (Fig. 2). We measure a total transmission loss (Lt) of 3.49 dB, 3.73 dB, 4.36 dB, and 4.30 dB in the four waveguide loops for the 8-fiber array. We monitor the amount of optical loss through the photonic chip by first measuring the input loss on the fiber connector side and then measuring the optical loss at the cleaved fiber array side to be 0.15 dB. This is the cleaved fiber-array to connector loss (Lc) per optical fiber in a loop. To measure the waveguide propagation loss, we compare the throughput of a straight waveguide while collecting the output with a lens to that of collecting the output with a second fiber. The waveguide propagation loss (Lw) through the looped waveguide is 0.40 dB. The total transmission loss can be defined as the sum of waveguide propagation loss, two times the fiber to connector loss, and two times the coupling loss per-facet(C) $L_t = L_w + 2L_c + 2C$. After subtracting the waveguide propagation loss per connection, we measure the loss through the loops of -3.09 dB, -3.33 dB, -3.96 dB and -3.90 dB, respectively. We subtract the fiber connector loss for each loop (0.3 dB) and get the loss through the loops as -2.79 dB, -3.03 dB, -3.66 dB and -3.60 dB, respectively. To obtain the per-facet coupling loss we divide this value by 2, which represents an average loss between the two facets. We calculate the per-facet coupling loss for the 4 loops as -1.40 dB, -1.50 dB, -1.78 dB, and -1.80 dB, respectively. We follow the same process for 4-fiber and 2-fiber arrays. We measure a variation of 0.00 dB across the 4-fiber array at 1550 nm and of +/- 0.20 dB through the 8-fiber array at 1550 nm as shown in Fig. 5. We

also measure a ± 0.40 dB variation in output power as a function of wavelength in the S, C, and L bands throughout 1480 nm to 1640 nm with the lowest loss of 0.80 dB for a 2-fiber array as shown in Fig. 5.b. These loss values are the best among multiple measurements with a typical insertion loss of <2 dB for an 8-fiber array. The increase in loss for an 8-fiber array is due to the variation in the eccentricity of the cores. We expect to see a decrease in the coupling loss if an optical adhesive, applied after the fusion, is used for optimum mode matching [21,28].

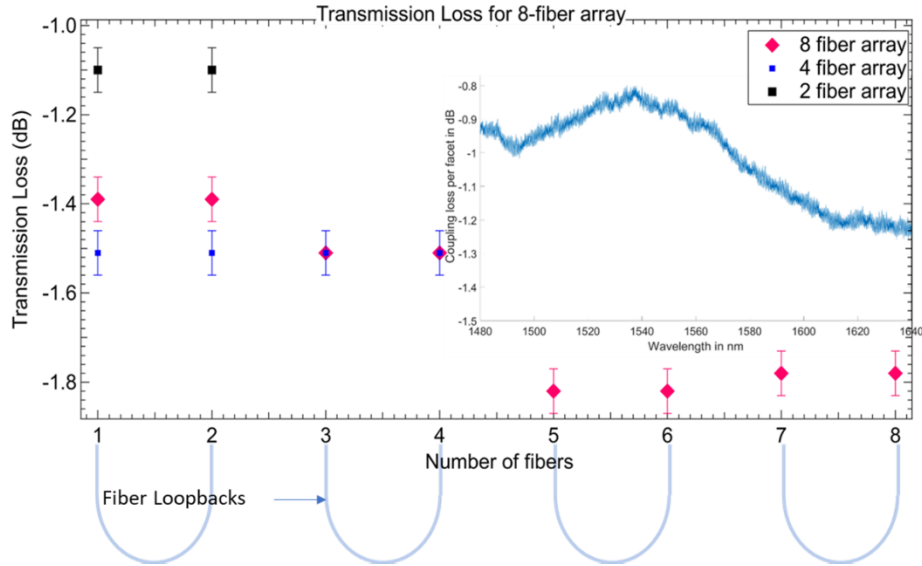


Fig. 5. (a) Transmission loss for a 2, 4, and 8 fiber-array after fusion splicing, (b) and variation of coupling loss as a function of wavelength from 1480 nm to 1640 nm (inset)

We experimentally measure an improvement of 1.85 dB per facet with the introduction of silicon dioxide mode converters at the end of a silicon nitride inverse taper when compared to using only a waveguide nanotaper as shown in Table 1. We fabricate two sets of devices, one with a set of oxide mode converters and the other without a mode converter, to measure the improvement in performance with the introduction of the mode converters. This provides us with a reference measurement of edge coupled fiber to a silicon nitride nanotaper compared to a separate chip with the same silicon nitride nanotaper but with the addition of the mode converter. We keep the input and output fibers the same to remove variations in loss from optical fiber connectors. We measure the transmission loss through a single loopback including the loss from the waveguide as -3.61 dB for a chip without the mode converter and -1.76 dB with a mode converter as shown in Table 1.

Table 1. Improvement in coupling loss with the introduction of oxide mode converter

	Without mode converter dB	With mode converter dB	Improvement dB
Coupling Loss	-3.61	-1.76	-1.85

Multiple fiber-to-chip fusion splicing has the potential to enable high throughput optical packaging with a robust, high efficiency, and low-cost solution. Packaging of multiple fibers in a single shot significantly increases the throughput of photonic packaging. The laser fusion splicing method enables optical packaging of photonic devices without the use of adhesives making them robust and tolerant to environmental fluctuations. The method is compatible with multiple photonic platforms, such as silicon, silicon nitride, aluminum nitride, and lithium niobate, which

use silicon dioxide as cladding. We envision that this method can be fully automated to enable highly efficient fiber-to-chip coupling in high-volume applications and can be extended to passive alignment techniques.

Funding. National Science Foundation (TI2140871).

Acknowledgments. This work was performed in part at the Cornell NanoScale Facility, a member of the National Nanotechnology Coordinated Infrastructure (NNCI), which is supported by the National Science Foundation (Grant NNCI-2025233). The authors appreciate the staff at these facilities for their help with equipment during the preparation of the samples. Portions of this work were presented at the {conference name} in {year}, {paper number or paper title}

Disclosures. J. Nauriyal and J. Cardenas declare the following competing interests: They are founders of and hold a financial stake in Photonect Interconnect Solutions Inc, a company commercializing the technology described in this article.

Data availability. Data underlying the results presented in this paper are available from the corresponding author by reasonable request.

References

1. R. Stone, R. Chen, J. Rahn, S. Venkataraman, X. Wang, K. Schmidtke, and J. Stewart, "Co-packaged Optics for Data Center Switching," in *European Conference on Optical Communications* (2020), pp. 1–3.
2. C. Kopp, S. Bernabé, B. B. Bakir, J. Fedeli, R. Orobouch, F. Schrank, H. Porte, L. Zimmermann, and T. Tekin, "Silicon Photonic Circuits: On-CMOS Integration, Fiber Optical Coupling, and Packaging," *IEEE J. Sel. Top. Quantum Electron.* **17**(3), 498–509 (2011).
3. D. Kuchta, M. Meghelli, and P. Pepeljugoski, *et al.*, "An 800 Gb/s, 16 channel, VCSEL-based, co-packaged transceiver with fast laser sparing," in *European Conference on Optical Communication* (Optica Publishing Group, 2022), paper Tu1F.2.
4. R. Mahajan, X. Li, and J. Fryman, *et al.*, "Co-Packaged Photonics For High Performance Computing: Status, Challenges And Opportunities," *J. Lightwave Technol.* **40**(2), 379–392 (2022).
5. M. Glick, L. C. Kimmerling, and R. C. Pfahl, "A Roadmap for Integrated Photonics," *Opt. Photonics News* **29**(3), 36 (2018).
6. C. Scarella, K. Gradkowski, L. Carroll, J.-S. Lee, M. Duperron, D. Fowler, and P. O'Brien, "Pluggable Single-Mode Fiber-Array-to-PIC Coupling Using Micro-Lenses," *IEEE Photonics Technol. Lett.* **29**(22), 1943–1946 (2017).
7. F. E. Doany, B. G. Lee, S. Assefa, W. M. J. Green, M. Yang, C. L. Schow, C. V. Jahnes, S. Zhang, J. Singer, V. I. Kopp, J. A. Kash, and Y. A. Vlasov, "Multichannel High-Bandwidth Coupling of Ultradense Silicon Photonic Waveguide Array to Standard-Pitch Fiber Array," *J. Lightwave Technol.* **29**(4), 475–482 (2011).
8. T. Barwicz, T. W. Lichoulas, Y. Taira, Y. Martin, S. Takenobu, A. Janta-Polczynski, H. Numata, E. L. Kimbrell, J.-W. Nah, B. Peng, D. Childers, R. Leidy, M. Khater, S. Kamlapurkar, E. Cyr, S. Engelmann, P. Fortier, and N. Boyer, "Automated, high-throughput photonic packaging," *Opt. Fiber Technol.* (2018).
9. T. Barwicz, Y. Taira, T. W. Lichoulas, N. Boyer, Y. Martin, H. Numata, J.-W. Nah, S. Takenobu, A. Janta-Polczynski, E. L. Kimbrell, R. Leidy, M. H. Khater, S. Kamlapurkar, S. Engelmann, Y. A. Vlasov, and P. Fortier, "A Novel Approach to Photonic Packaging Leveraging Existing High-Throughput Microelectronic Facilities," *IEEE J. Sel. Top. Quantum Electron.* **22**(9), 455–466 (2016).
10. T. Tekin, "Review of Packaging of Optoelectronic, Photonic, and MEMS Components," *IEEE J. Sel. Top. Quantum Electron.* **17**(3), 704–719 (2011).
11. I.-L. Bundalo, P. E. Morrissey, and A. Annoni, *et al.*, "PIXAPP Photonics Packaging Pilot Line – Development of a Silicon Photonic Optical Transceiver With Pluggable Fiber Connectivity," *IEEE J. Sel. Top. Quantum Electron.* **28**(3), 1–11 (2022).
12. L. Carroll, J.-S. Lee, C. Scarella, K. Gradkowski, M. Duperron, H. Lu, Y. Zhao, C. Eason, P. Morrissey, M. Rensing, S. Collins, H. Y. Hwang, and P. O'Brien, "Photonic Packaging: Transforming Silicon Photonic Integrated Circuits into Photonic Devices," *Appl. Sci.* **6**(12), 426 (2016).
13. B. Snyder and P. O'Brien, "Packaging Process for Grating-Coupled Silicon Photonic Waveguides Using Angle-Polished Fibers," *IEEE Trans. Compon., Packag. Manufact. Technol.* **3**(6), 954–959 (2013).
14. B. Snyder and P. O'Brien, "Planar Fiber Packaging Method for Silicon Photonic Integrated Circuits," in *Optical Fiber Communication Conference* (Optical Society of America, 2012), paper OM2E.5.
15. N. Pavarelli, J. S. Lee, M. Rensing, C. Scarella, S. Zhou, P. Ossieur, and P. A. OBrien, "Optical and Electronic Packaging Processes for Silicon Photonic Systems," *J. Lightwave Technol.* **33**(5), 991–997 (2015).
16. R. Selim, R. Hoofman, R. Labie, V. Sandeep, T. Drischel, and K. Torki, "Scale Up Of Advanced Packaging And System Integration For Hybrid Technologies," in *Smart Systems Integration* (2021), pp. 1–4.
17. A. Janta-Polczynski, E. Cyr, R. Langlois, P. Fortier, Y. Taira, N. Boyer, and T. Barwicz, "Solder-Reflowable, High-Throughput Fiber Assembly Achieved by Partitioning of Adhesive Functions," in *68th Electronic Components and Technology Conference* (IEEE, 2018), pp. 1109–1117.
18. T. Barwicz, E. Kimbrell, and T. Lichoulas, "Dual-polymer fiber optic interface with melt-bond adhesive," United States patent US9360635B2 (June 7, 2016).

19. K. Gilleo, "Photonics challenge to electronic packaging," *IEEE Trans. Compon. Packag. Technol.* **24**(2), 309–311 (2001).
20. M. A. Uddin, H. P. Chan, K. W. Lam, Y. C. Chan, P. L. Chu, K. C. Hung, and T. O. Tsun, "Delamination problems of UV-cured adhesive bonded optical fiber in V-groove for photonic packaging," *IEEE Photonics Technol. Lett.* **16**(4), 1113–1115 (2004).
21. J. Nauriyal, M. Song, R. Yu, and J. Cardenas, "Fiber-to-chip fusion splicing for low-loss photonic packaging," *Optica* **6**(5), 549–552 (2019).
22. S. Park, J.-M. Lee, and S. C. Ko, "Fabrication method for passive alignment in polymer PLCs with U-grooves," *IEEE Photonics Technol. Lett.* **17**(7), 1444–1446 (2005).
23. V. R. Almeida, R. R. Panepucci, and M. Lipson, "Nanotaper for compact mode conversion," *Opt. Lett.* **28**(15), 1302–1304 (2003).
24. P. Pal and W. H. Knox, "Low loss fusion splicing of micron scale silica fibers," *Opt. Express* **16**(15), 11568–11573 (2008).
25. N. Shimizu, "Fusion splicing between deposited silica waveguides and optical fibers," *Electron. Commun. Jpn. Part Commun.* **67**, 115–122 (n.d.).
26. N. Shimizu, N. Imoto, and M. Ikeda, "Fusion splicing between optical circuits and optical fibres," *Electron. Lett.* **19**(3), 96–97 (1983).
27. J. Nauriyal, Y. Zhang, M. Song, and J. Cardenas, "Low-loss, Single-shot Fiber-Array to Chip Attach Using Laser Fusion Splicing," in *Photonics Conference* (IEEE, 2022), pp. 1–2.
28. L. Chen, C. R. Doerr, Y.-K. Chen, and T.-Y. Liow, "Low-Loss and Broadband Cantilever Couplers Between Standard Cleaved Fibers and High-Index-Contrast Si N or Si Waveguides," *IEEE Photonics Technol. Lett.* **22**(23), 1744–1746 (2010).